DOI: 10.1002/ange.201300431

Drug Delivery

Biodegradable ZnO@polymer Core–Shell Nanocarriers: pH-Triggered Release of Doxorubicin In Vitro**

Zheng-Yong Zhang, Yu-Dong Xu, Ying-Ying Ma, Li-Li Qiu, Yi Wang, Ji-Lie Kong, and Huan-Ming Xiong**

In the past decades, drug delivery systems (DDSs) based on nanotechnology have been studied extensively to overcome the nonselectivity of chemotherapy, to avoid damaging healthy tissues, and to improve cancer cure rates.[1–3] A practical DDS should possess the two general characteristics of specific targeting and controllable release. With regard to specific targeting, it is widely accepted that nanocarriers are able to enter cells rapidly through intracellular endocytic pathways[4] and effectively release drugs at target sites. With regard to controllable release, different responding agents or conditions have been employed, such as pH,[5] temperature,[6] enzyme,[7,8] biomolecules[9,10] and light.[11–13] Among these, pH-responsive DDSs have shown great advantages as a result of their simple design and universal applicability, because pH values in tumors and inflammatory tissues are significantly lower than those in blood and normal tissues.[14–16] The pH-responsive systems usually employ pH-sensitive linkers,[17] pH-responsive polymeric micelles,[18] pH-tunable calcium phosphate,[19] etc. For instance, pH-responsive molecules[20] or ZnO nanoparticles[21] can be used as cappers to cover the pores of mesoporous silica nanoparticles (MSNs). However, the strong adsorption ability of MSNs hinders the complete release of the drug and the biodegradability of MSNs also remains a controversial problem.[22] As we reported previously, these problems cannot be resolved by using nanocarriers based on carbon nanotubes and mesoporous carbon materials.[23,24]

As a cheap nanomaterial with low toxicity, ZnO quantum dots (QDs) have shown great potential for application in bioimaging.[25–28] Because the unprotected ZnO QDs are decomposed completely at pH 5 in aqueous solution, these materials can be employed as nanocarriers for drug delivery. Herein, we synthesized biodegradable ZnO@polymer core–shell QDs with excellent water solubility, biocompatibility, and pH sensitivity as drug carriers in order to study the release process and activity in vitro. Polyacrylamide, which is nontoxic to animals,[29] was used as a protecting shell for the ZnO QDs. The well-known doxorubicin hydrochloride (DOX) was selected as anticancer drug because its clinical application has so far been hampered by nonselective biodistribution and severe damage to healthy tissues.[30] Furthermore, human glioblastoma cells (U251), the most common cells in malignancies of the human brain,[31] were chosen as model cells. DOX is a hydrophilic molecule and its ability to pass through biological barriers such as the blood–brain barrier is rather weak, hence treatment of brain tumors with DOX remains a challenge.[32] After they were loaded with DOX, our ZnO@polymer QDs crossed the cell membrane through a cellular uptake pathway, decomposed at the endosomes or lysosomes to release DOX molecules, which finally penetrated into the nuclei to kill the cells. This process and the drug release mechanism were proven by direct observation under a confocal laser scanning microscope.

We developed a two-step copolymerization method for the synthesis of core–shell-structured ZnO@polymer QDs with stable luminescence in aqueous solutions.[25,33] The obtained 3 nm-sized ZnO@polymer can load DOX to form a ZnO@polymer–DOX nanocomposite (see the Supporting Information). The luminescence of an aqueous solution of ZnO@polymer (Figure 1 A) is green under irradiation with UV light, and the corresponding quantum yield (QY) is nearly 40 % using rhodamine 6G as a reference[25,26] (QY = 95 % in ethanol). The absorption onset and excitation peak are at about 330 nm, while the wavelength of the green emission is around 520 nm, which is typical for ZnO defects. The absorption band maximum of DOX is at 500 nm and wavelength of the red emission is around 595 nm (Figure 1 B). After adding ZnO@polymer QDs to an aqueous solution of DOX, the UV/Vis absorption spectra and the photoluminescence (PL) spectra in Figure 1 C show the mixed features of both Figure 1 A and Figure 1 B, thus indicating that both ZnO@polymer and DOX are stabilized in the nanocomposites. Moreover, the PL emission band of DOX is enhanced significantly, although the excitation wavelength of 330 nm is chosen for ZnO, which can be attributed to the fluorescence resonance energy transfer (FRET) from the ZnO to DOX.

[*] Y.-D. Xu, Y.-Y. Ma, L.-L. Qiu, Prof. H.-M. Xiong
Department of Chemistry and Shanghai Key Laboratory of Molecular Catalysis and Innovative Materials
Fudan University
Shanghai, 200433 (P.R. China)
E-mail: hmxiong@fudan.edu.cn
Dr. Z.-Y. Zhang, Prof. J.-L. Kong
Department of Chemistry and Institutes of Biomedical Sciences, Fudan University
Shanghai, 200433 (P.R. China)
E-mail: jlkong@fudan.edu.cn
Dr. Y. Wang
Department of Chemistry and Center of Analysis and Measurement, Fudan University
Shanghai 200433 (P.R. China)

[**] This work was supported by the National Natural Science Foundation of China (20890022, 21175029, 21271045), the National Basic Research Program of China (2013CB934102), NCET-11-0115, and the Shanghai Leading Academic Discipline Project (B109).

Supporting information for this article is available on the WWW under http://dx.doi.org/10.1002/anie.201300431.

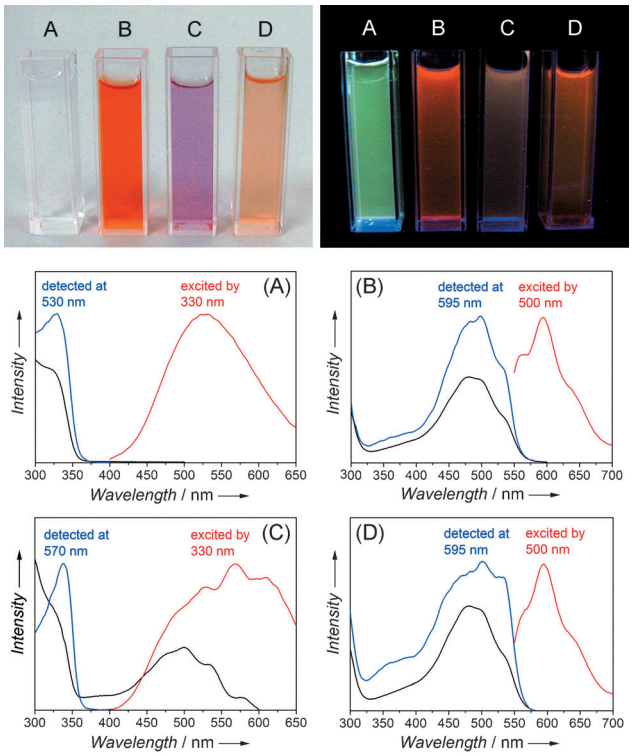

Figure 1. Top: Photographs of aqueous solutions of A) ZnO@polymer, B) free DOX, C) ZnO@polymer–DOX nanoparticles, and D) DOX released from ZnO@polymer–DOX at pH 5.0 under white light (left) and UV light (320 nm; right). Bottom: UV/Vis absorption spectra (black), excitation (blue), and emission (red) fluorescence spectra of these samples.

However, after the release of DOX by acid, the color of the mixture changed back to red, and the corresponding UV/Vis absorption and PL spectra in Figure 1 D are similar to those in Figure 1 B, thus proving that ZnO@polymer decomposes at pH 5.0, while DOX is stable at this pH. This result confirms that the DOX molecules have been released from the surfaces of the nanoparticles after treatment with acid.

This pH-responsive behavior of ZnO@polymer–DOX was studied by UV/Vis absorption spectroscopy. The UV/Vis absorption around 330 nm, which corresponds to the band gap of ZnO, becomes weaker and weaker when the pH value of the solution changes from 7.0 to 5.0 (Figure 2 A). In contrast, DOX is stable during the change of the pH value, and the corresponding UV/Vis absorption band at about 500 nm shows almost no change. The release profile of DOX from ZnO@polymer–DOX at different pH values shows that about 15 wt. % of DOX were released after 10 h at pH 7.0, but no more DOX was released in the subsequent 30 h (Figure 2 B). We speculate that 15 wt. % of the DOX molecules were adsorbed weakly on the surface of the nanoparticles, while the remaining DOX molecules were adhered chemically on the nanocomposite. In contrast, nearly 90 wt. % of DOX molecules were released within 10 h at pH 5.0, and a little more DOX was released slowly and continuously after that time, which could be ascribed to the adsorption effects between DOX and the polymer shell. Therefore, our ZnO@polymer–DOX is a pH-responsive, degradable system for DOX delivery and suitable for the specific targeting at solid tumors.[34]

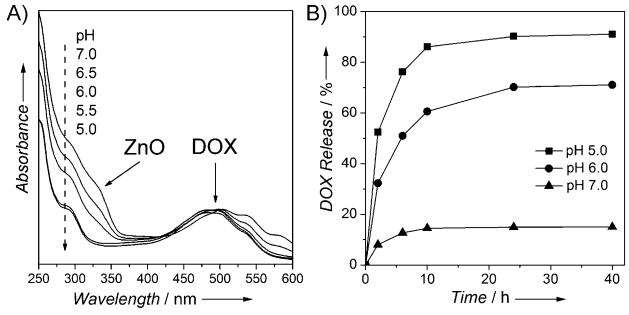

Figure 2. A) UV/Vis absorption spectra of aqueous solutions of ZnO@polymer–DOX with a decreasing pH value from 7.0 to 5.0. B) DOX release profile of ZnO@polymer–DOX at different pH values.

The cytotoxicities of ZnO@polymer, DOX, and ZnO@polymer–DOX were assessed by MTT assays (MTT = 3-(4,5-dimethylthiazol-2-yl)-2,5-diphenyltetrazolium bromide) after incubation with U251 cells for 48 h (Figure 3). The ZnO@polymer nanoparticles have no visible cytotoxic effect on U251 cells after 48 h treatment, even at a concentration of 7.5 $\mu g\,mL^{-1}$ (Zn content), and the cytotoxicity of ZnO nanoparticles is mainly attributed to the zinc ions that were released from the nanoparticles after dissolution.[35–37] In contrast, the cytotoxicity of DOX is significant at a small concentration of 0.5 $\mu g\,mL^{-1}$. Although both free DOX and ZnO@polymer–DOX exhibit dose-dependent cytotoxicity toward cancer cells, the cytotoxicity of DOX does not increase significantly when its concentration is over 1 $\mu g\,mL^{-1}$, while ZnO@polymer–DOX exhibits much stronger cytotoxicity when its DOX concentration is over 2 $\mu g\,mL^{-1}$ (DOX content). As a result, ZnO@polymer–DOX is able to kill cancer cells effectively at appropriate concentrations (see right columns in Figure 3), and the side effects of chemotherapy are suppressed simultaneously. This phenomenon can be ascribed to the cytotoxicity enhancement effects of the nanocarriers, which result in the improved

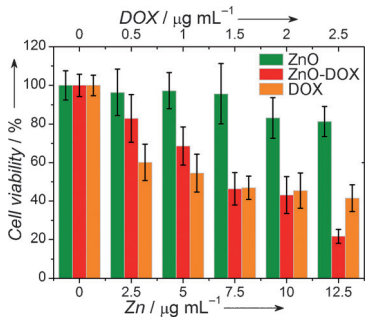

Figure 3. Viability of U251 cells after treatment with ZnO@polymer QDs, ZnO@polymer–DOX composites, and free DOX for 48 h. The cytotoxicity of ZnO@polymer and ZnO@polymer–DOX were evaluated with regard to their Zn content (see the lower scale mark). The cytotoxicity of DOX and ZnO@polymer–DOX were evaluated with regard to their DOX content (see the upper scale mark).

internalization of ZnO@polymer–DOX through endocytosis compared with the passive diffusion of free DOX into cells.[38]

Recently, ZnO nanomaterials were investigated as a platform for DOX delivery.[39–41] Although some related pH-controlled experiments were conducted to suggest a possible mechanism, the authors did not provide detailed proof for the cell-entering process of ZnO–DOX, the decomposition at lysosomes, and the release of DOX into the nucleus. Herein, we proved this process by confocal laser scanning microscopy (CLSM) images with high resolution. After 3 h incubation, red fluorescence from DOX can be found throughout the cytoplasm and localizes especially in the lysosomes labeled by LysoTracker Green (see the yellow points in Figure 4C). At

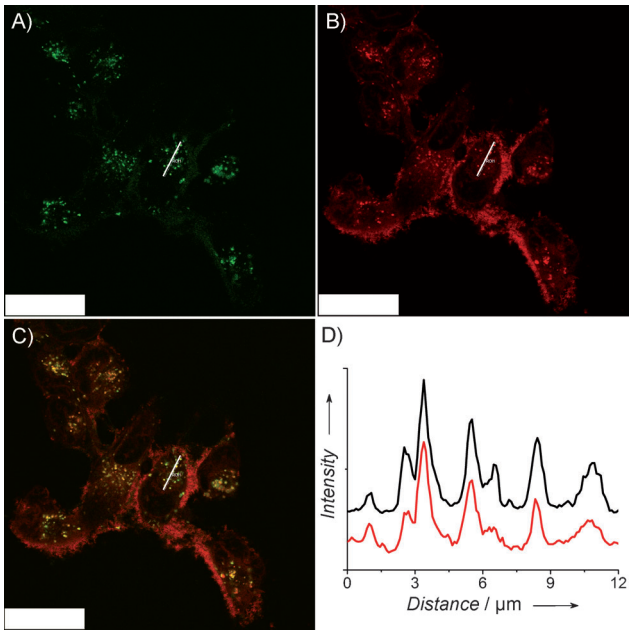

Figure 4. CLSM images of U251 cells after incubation with ZnO@polymer–DOX in the presence of LysoTracker for 3 h. A) Lysosomes stained with LysoTracker (green). B) ZnO@polymer–DOX (red). C) Merged picture of the above two channels. Scale bars = 25 μm. D) Fluorescence signals of lysosomes (black) and ZnO@polymer–DOX (red) based on the white lines in images A and B, respectively.

the cellular level, the internalization of most nanoparticles will occur through the cellular endocytic pathway, that is, after being engulfed by cells, the nanoparticles are trafficked into the early endosomes, then into the late endosomes/lysosomes, and finally fused with lysosomes. Both endosomes (pH 5.0–6.0) and lysosomes (pH 4.5–5.0) have an acidic microenvironment, which is distinct from that outside the cells (pH 7.4).[42–44] The fluorescence signals from Figure 4A and Figure 4B match well (Figure 4D), thus confirming that plenty of ZnO@polymer–DOX nanoparticles are decomposed in the lysosomes.

We further used Zinquin ethyl ester, a zinc-specific fluorescent dye, to investigate the accumulation of zinc ions in the cells. The control sample (without incubation with any other reagent or nanomaterial) only shows very weak blue fluorescence (Figure 5), because zinc salts are indispensable

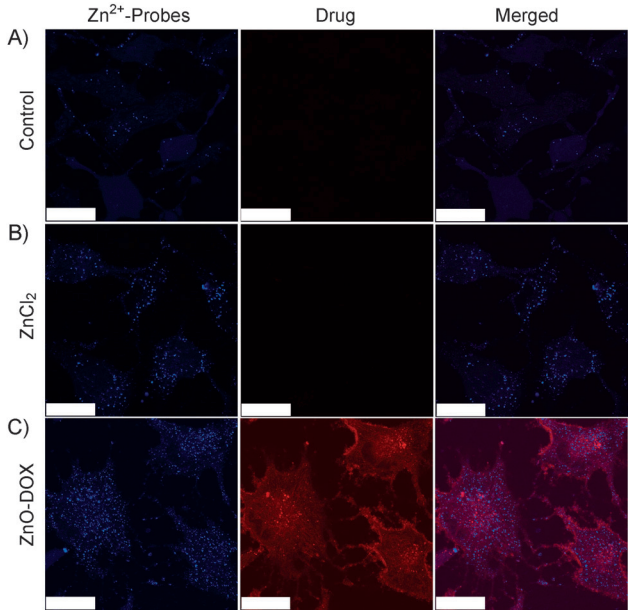

Figure 5. CLSM images of U251 cells after incubation with A) no agents, B) $ZnCl_2$, and C) ZnO@polymer–DOX for 24 h. The Zn ions was stained with fluorescent Zinquin ethyl ester (blue). Scale bars = 25 μm.

components of the cell culture medium. For comparison, the cells treated with $ZnCl_2$ exhibit bright blue color. In the cells treated with ZnO@polymer–DOX, the blue fluorescence is significantly stronger than that of the control, thus confirming the biodegradation of the ZnO@polymer–DOX nanocarriers. It is interesting that in the merged picture, the blue points of Zinquin ethyl ester and the red points of DOX do not overlap (as in Figure 4C), thus indicating that the released Zn^{II} ions are enriched in vesicles called zincosomes (containing high amounts of labile zinc),[45–47] while DOX molecules mainly locate in the cytoplasm. Figure S7 and Videos S1–S9 show the drug delivery process in a dynamic fashion, and the results clearly show that the blue fluorescence of Zinquin arises from ionic Zn^{2+}.

The cellular uptake of ZnO@polymer–DOX was verified by CLSM photographs of cancer cells that were incubated with the nanocomposites for 3, 24, and 48 h (Figure 6). After incubation for 3 h, there was only a low accumulation of DOX in the cytoplasm and even less in the nucleus. Although some ZnO@polymer–DOX was taken up by cells in the first 3 h, the release of DOX from the nanocarriers was delayed by biodegradation in endosomes/lysosomes and the traffic process. After incubation for 24 h, bright-red-emitting DOX was observed in both the cytoplasm and the nucleus of the cell, thus indicating that ZnO@polymer–DOX had decomposed and the released DOX molecules had accumulated around and finally entered the nucleus. After incubation for 48 h, most of the DOX molecules were released from the nanocarriers and located in the cell nucleus. It is known that the main target site of DOX is the cell nucleus, where DOX can attach to double-stranded DNA to form DNA adducts, thus inhibiting the activity of topoisomerase and inducing cell death (apoptosis).[48] All the above results suggest that the

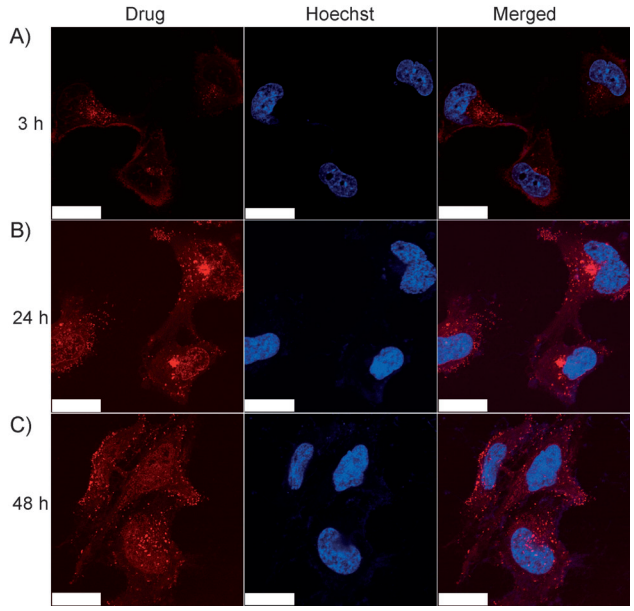

Figure 6. CLSM images of U251 cells that were incubated with ZnO@polymer–DOX nanocomposites for 3, 24, and 48 h at 37 °C. Each series contains the drug (red), the nuclei of the cells (dyed blue with Hoechst 33342), and the merged picture of the two channels, respectively. Scale bars = 25 μm.

drug delivery mechanism includes the cellular internalization of ZnO@polymer–DOX, followed by its biodegradation in endosomes/lysosomes, and the subsequent penetration of the drug into the nucleus.

In summary, we have successfully developed a nanocomposite-based drug-delivery system, using human glioblastoma cells as the model, thus suggesting the treatment of brain cancer as a potential application. In comparison with previously reported nanocomposite-based DOX-release systems, our system has three advantages. First, the ZnO@polymer QDs are very stable in aqueous solution at pH 7.0, but rapidly decompose at pH 6.0, thus ensuring the safety of healthy tissues. Secondly, both ZnO and the polymer shell are biodegradable and thus safe for cells, and the ZnO@polymer is nontoxic to U251 cells at low concentrations, but shows high cytotoxicity after DOX loading. As a result, ZnO@polymer–DOX in an appropriate concentration and composition can be used to realize therapeutic effectiveness and avoid systemic toxicity simultaneously. Thirdly, because DOX is photoluminescent, and the decomposed ZnO@polymer is not, we were able to use LysoTracker and Zinquin ethyl ester to track the drug delivery process by CLSM, and to finally disclose the whole mechanism.

Received: January 17, 2013
Published online: March 5, 2013

Keywords: chemotherapy · doxorubicin · drug delivery · nanoparticles · zinc oxide

[1] R. A. Petros, J. M. DeSimone, *Nat. Rev. Drug Discovery* **2010**, *9*, 615 – 627.
[2] L. Zhang, F. X. Gu, J. M. Chan, A. Z. Wang, R. S. Langer, O. C. Farokhzad, *Clin. Pharmacol. Ther.* **2008**, *83*, 761 – 769.
[3] K. Riehemann, S. W. Schneider, T. A. Luger, B. Godin, M. Ferrari, H. Fuchs, *Angew. Chem.* **2009**, *121*, 886 – 913; *Angew. Chem. Int. Ed.* **2009**, *48*, 872 – 897.
[4] F. Zhao, Y. Zhao, Y. Liu, X. L. Chang, C. Y. Chen, Y. L. Zhao, *Small* **2011**, *7*, 1322 – 1337.
[5] J. Z. Du, X. J. Du, C. Q. Mao, J. Wang, *J. Am. Chem. Soc.* **2011**, *133*, 17560 – 17563.
[6] J. Croissant, J. I. Zink, *J. Am. Chem. Soc.* **2012**, *134*, 7628 – 7631.
[7] K. Patel, S. Angelos, W. R. Dichtel, A. Coskun, Y. W. Yang, J. I. Zink, J. F. Stoddart, *J. Am. Chem. Soc.* **2008**, *130*, 2382 – 2383.
[8] A. Bernardos, L. Mondragón, E. Aznar, M. D. Marcos, R. Martínez-Máñez, F. Sancenón, J. Soto, J. M. Barat, E. Pérez-Payá, C. Guillem, P. Amorós, *ACS Nano* **2010**, *4*, 6353 – 6368.
[9] Y. N. Zhao, B. G. Trewyn, I. I. Slowing, V. S.-Y. Lin, *J. Am. Chem. Soc.* **2009**, *131*, 8398 – 8400.
[10] S. Santra, C. Kaittanis, O. J. Santiesteban, J. M. Perez, *J. Am. Chem. Soc.* **2011**, *133*, 16680 – 16688.
[11] V. Voliani, F. Ricci, G. Signore, R. Nifosì, S. Luin, F. Beltram, *Small* **2011**, *7*, 3271 – 3275.
[12] N. Ž. Knežević, B. G. Trewyn, V. S.-Y. Lin, *Chem. Eur. J.* **2011**, *17*, 3338 – 3342.
[13] W. J. Fang, J. Yang, J. W. Gong, N. F. Zheng, *Adv. Funct. Mater.* **2012**, *22*, 842 – 848.
[14] J. Z. Du, T. M. Sun, W. J. Song, J. Wu, J. Wang, *Angew. Chem.* **2010**, *122*, 3703 – 3708; *Angew. Chem. Int. Ed.* **2010**, *49*, 3621 – 3626.
[15] Y. P. Li, W. W. Xiao, K. Xiao, L. Berti, J. T. Luo, H. P. Tseng, G. Fung, K. S. Lam, *Angew. Chem.* **2012**, *124*, 2918 – 2923; *Angew. Chem. Int. Ed.* **2012**, *51*, 2864 – 2869.
[16] D. Li, J. Tang, C. Wei, J. Guo, S. L. Wang, D. Chaudhary, C. C. Wang, *Small* **2012**, *8*, 2690 – 2697.
[17] R. Liu, Y. Zhang, X. Zhao, A. Agarwal, L. J. Mueller, P. Y. Feng, *J. Am. Chem. Soc.* **2010**, *132*, 1500 – 1501.
[18] X. B. Xiong, A. Lavasanifar, *ACS Nano* **2011**, *5*, 5202 – 5213.
[19] H. P. Rim, K. H. Min, H. J. Lee, S. Y. Jeong, S. C. Lee, *Angew. Chem.* **2011**, *123*, 9015 – 9019; *Angew. Chem. Int. Ed.* **2011**, *50*, 8853 – 8857.
[20] Y. L. Zhao, Z. X. Li, S. Kabehie, Y. Y. Botros, J. F. Stoddart, J. I. Zink, *J. Am. Chem. Soc.* **2010**, *132*, 13016 – 13025.
[21] F. Muhammad, M. Y. Guo, W. X. Qi, F. X. Sun, A. F. Wang, Y. J. Guo, G. S. Zhu, *J. Am. Chem. Soc.* **2011**, *133*, 8778 – 8781.
[22] Y. S. Lin, K. R. Hurley, C. L. Haynes, *J. Phys. Chem. Lett.* **2012**, *3*, 364 – 374.
[23] J. Zhu, L. Liao, X. J. Bian, J. L. Kong, P. Y. Yang, B. H. Liu, *Small* **2012**, *8*, 2715 – 2720.
[24] M. Y. Wang, S. N. Yu, C. Wang, J. L. Kong, *ACS Nano* **2010**, *4*, 6483 – 6490.
[25] H. M. Xiong, Y. Xu, Q. G. Ren, Y. Y. Xia, *J. Am. Chem. Soc.* **2008**, *130*, 7522 – 7523.
[26] H. M. Xiong, D. G. Shchukin, H. Möhwald, Y. Xu, Y. Y. Xia, *Angew. Chem.* **2009**, *121*, 2765 – 2769; *Angew. Chem. Int. Ed.* **2009**, *48*, 2727 – 2731.
[27] Z. Y. Pan, J. Liang, Z. Z. Zheng, H. H. Wang, H. M. Xiong, *Contrast Media Mol. Imaging* **2011**, *6*, 328 – 330.
[28] H. J. Zhang, H. M. Xiong, Q. G. Ren, Y. Y. Xia, J. L. Kong, *J. Mater. Chem.* **2012**, *22*, 13159 – 13165.
[29] M. J. Caulfield, G. G. Qiao, D. H. Solomon, *Chem. Rev.* **2002**, *102*, 3067 – 3083.
[30] L. J. Meng, X. K. Zhang, Q. H. Lu, Z. F. Fei, P. J. Dyson, *Biomaterials* **2012**, *33*, 1689 – 1698.
[31] D. A. Daniels, H. Chen, B. J. Hicke, K. M. Swiderek, L. Gold, *Proc. Natl. Acad. Sci. USA* **2003**, *100*, 15416 – 15421.

[32] S. Dhar, E. M. Reddy, A. Shiras, V. Pokharkar, B. L. V. Prasad, *Chem. Eur. J.* **2008**, *14*, 10244 – 10250.
[33] H. M. Xiong, *J. Mater. Chem.* **2010**, *20*, 4251 – 4262.
[34] Y. L. Dai, P. A. Ma, Z. Y. Cheng, X. J. Kang, X. Zhang, Z. Y. Hou, C. X. Li, D. M. Yang, X. F. Zhai, J. Lin, *ACS Nano* **2012**, *6*, 3327 – 3338.
[35] K. H. Müller, J. Kulkarni, M. Motskin, A. Goode, P. Winship, J. N. Skepper, M. P. Ryan, A. E. Porter, *ACS Nano* **2010**, *4*, 6767 – 6779.
[36] T. Xia, M. Kovochich, M. Liong, L. Mädler, B. Gilbert, H. B. Shi, J. I. Yeh, J. I. Zink, A. E. Nel, *ACS Nano* **2008**, *2*, 2121 – 2134.
[37] A. E. Nel, L. Mädler, D. Velegol, T. Xia, E. M. V. Hoek, P. Somasundaran, F. Klaessig, V. Castranova, M. Thompson, *Nat. Mater.* **2009**, *8*, 543 – 557.
[38] S. C. J. Steiniger, J. Kreuter, A. S. Khalansky, I. N. Skidan, A. I. Bobruskin, Z. S. Smirnova, S. E. Severin, R. Uhl, M. Kock, K. D. Geiger, S. E. Gelperina, *Int. J. Cancer* **2004**, *109*, 759 – 767.
[39] Q. Yuan, S. Hein, R. D. K. Misra, *Acta Biomater.* **2010**, *6*, 2732 – 2739.
[40] K. C. Barick, S. Nigam, D. Bahadur, *J. Mater. Chem.* **2010**, *20*, 6446 – 6452.
[41] F. Muhammad, M. Y. Guo, Y. J. Guo, W. X. Qi, F. Y. Qu, F. X. Sun, H. J. Zhao, G. S. Zhu, *J. Mater. Chem.* **2011**, *21*, 13406 – 13412.
[42] H. Shi, X. X. He, Y. Yuan, K. M. Wang, D. Liu, *Anal. Chem.* **2010**, *82*, 2213 – 2220.
[43] K. J. Zhou, H. M. Liu, S. R. Zhang, X. N. Huang, Y. G. Wang, G. Huang, B. D. Sumer, J. M. Gao, *J. Am. Chem. Soc.* **2012**, *134*, 7803 – 7811.
[44] C. J. Ke, T. Y. Su, H. L. Chen, H. L. Liu, W. L. Chiang, P. C. Chu, Y. N. Xia, H. W. Sung, *Angew. Chem.* **2011**, *123*, 8236 – 8239; *Angew. Chem. Int. Ed.* **2011**, *50*, 8086 – 8089.
[45] H. Haase, D. Beyersmann, *Biochem. Biophys. Res. Commun.* **2002**, *296*, 923 – 928.
[46] H. Haase, D. Beyersmann, *BioMetals* **1999**, *12*, 247 – 254.
[47] R. McRae, P. Bagchi, S. Sumalekshmy, C. J. Fahrni, *Chem. Rev.* **2009**, *109*, 4780 – 4827.
[48] S. Y. Han, Y. X. Liu, X. Nie, Q. Xu, F. Jiao, W. Li, Y. L. Zhao, Y. Wu, C. Y. Chen, *Small* **2012**, *8*, 1596 – 1606.

